Journal of Nanosciences: Current Research

Research Article Open Access

Biomimetic Synthesis and Characterization of Silver Nanoparticles Synthesized by Leaf Extract of *Bridellia stipularis* L Blume and Evaluation of their Effect on Mitotic Chromosomes of *Pisum Sativum* L

Azharuddin Daphedar and Tarikere C Taranath*

Department of Studies in Botany, Environmental Biology Laboratory, Karnatak University, Dharwad, Karnataka, India

Abstract

The present investigation focuses on the synthesis of silver nanoparticles using leaf extract of *Bridellia stipularis* and their effect on mitotic chromosomes of root meristem of *Pisum sativum*. The phytogenic silver nanoparticles were monitored by UV-Vis spectroscopy, FTIR, XRD, AFM and HR-TEM analysis. The ultraviolet-visible spectrum shows a prominent peak at λ_{max}=413 nm at pH 10. The size and shape of the AgNPs were found to be 5 to 85 nm and are spherical in nature. This study focuses on assessment of toxic effect of AgNPs on mitotic chromosomes of root meristematic cells of *P. sativum* (2n=14). *P. sativum* root cells were treated with four different concentrations 4, 8, 12, 16 µg/ml of the AgNPs solution at the interval of 6, 12, 18 and 24 hours duration. The mitotic index was decreased (55.43 ± 5.69% to 13.99 ± 0.60%) with an increase in the number of various chromosomal aberrations (36.95 ± 3.15%) at higher concentration. It is found that these chromosomal aberrations include chromatid bridge, sticky, diagonal chromosome, c-metaphase, multibridge and micronucleus. The results revealed that the percentage of mitotic index (MI) is inversely proportional and chromosomal aberrations (CAs) are directly proportional to the concentration and duration of exposure. The results were found to be statistically significant at $p<0.05$. It is evident from the results that AgNPs cause significant inhibition of mitotic index and increased chromosomal abnormalities.

Keywords: *Bridellia stipularis*; Silver nanoparticles; Cytotoxicity; Genotoxicity; *Pisum sativum* assay

Introduction

Over several decades, the noble metal nanoparticles have gained a lot of public interest due to increased application of nanomaterials within a size range of 1-100 nm in many areas of human endeavors [1]. Nowadays, nanotechnology is considered as the technology of 21st century, and it can be considered as an important bridge between nanotechnology and all available kinds of renewable energies [2-6]. The production of functional nanoparticles (gold, silver, zinc etc.) is versatile in the field of green nanotechnology [7]. Among them, silver nanoparticles are most widely used as anticancer, antioxidant, antifungal, antidiabetic,antiparasitic and antituberculosis agent [8-17]. Phytochemicals present in the leaf extract may act as both reducing and stabilizing agents for the synthesis of silver nanoparticles. These nanoparticles possess unique physical, chemical, electrical, magnetic, mechanical and biological properties [18]. Currently, metal nanoparticles are synthesized by various methods in high technological areas such as chemical [19-21], electrochemical [22], Magnetic and thermal properties [23], radiation [24], photochemical [25], and biological methods [26]. It was proved by many researchers that the exploiting nanofluid in solar systems, offers distinctive advantages over conventional fluids [27-29]. Nanofluids enhance the rate of heat transfer in many thermal generation industries. The physical and chemical methods have certain disadvantages due to involvement of hazardous by-products during their synthesis of nanomaterials and these chemicals pose a serious threat to the environment and human health. While, biological methods are reliable, cost-effective, environmentally benign, suitable for large scale production and these methods are more advantageous over the physicochemical methods [30-33]. Many investigators synthesized nanoparticles by using microorganisms [34], enzymes [35], fungi [36-38], and higher plants [39-42].

The *Bridelia stipularis* (L.) Blume plant species is used as a remedy for several diseases by traditional herbal healers for the treatment of jaundice, allergy, inflammation, scabies and anemia [43-46]. Because these plant species contain various medicinally important secondary metabolites and used for the production of anthocyanin pigments in plants [47]. In the present investigation, silver nanoparticles were synthesized by leaf extract of *B. stipularis* and used for the evaluation of their cytotoxicity on mitotic chromosomes of root meristems of *P. sativum* which serves as a genetic model system to study genetic endpoints like mitotic index (MI), chromosomal aberrations (CAs), nuclear abnormalities (NAs) and micronucleus (MN) in plant system [48]. The literature review reveals that there are no reports on cytotoxicity of silver nanoparticles on mitotic chromosomes of *P. sativum*.

Materials and methods

Plant material collection

The leaves of *B. stipularis* (synonym *Bridellia scandens*) belonging to the family Euphorbiaceae were collected from the Botanical Garden of Karnatak University campus, Dharwad, Karnataka India.

Preparation of aqueous leaf extract

The collected leaves of *B. Stipularis* were cleaned with running tap water to remove adhered dust impurities and other contaminants, followed by double-distilled de-ionized water and shade dried at room temperature. About 10 g of shade dried leaves were chopped into small pieces and transferred to 250 ml Erlenmeyer flask containing 100 ml of de-ionized water. Further, it was heated for 15-20 minutes

***Corresponding author:** Tarikere C Taranath, Department of Studies in Botany, Environmental Biology Laboratory, Karnatak University, Dharwad, Karnataka, India; E-mail: tctaranath@rediffmail.com

Received: March 04, 2019; **Accepted:** September 12, 2019; **Published:** September 25, 2019

Citation: Daphedar A, Taranath CT (2019) Biomimetic Synthesis and Characterization of Silver Nanoparticles Synthesized by Leaf Extract of *Bridellia stipularis* L Blume and Evaluation of their Effect on Mitotic Chromosomes of *Pisum Sativum* L. J Nanosci Curr Res 4: 132.

at 60˚C, until the color of the reaction mixture changes from watery to light yellow color. The aqueous extract was allowed to cool at room temperature and then filtered through Whatman no. 1 filter paper. The reaction mixture was stored in a refrigerator at 4˚C for further analysis.

Phytosynthesis of silver nanoparticles

Synthesis of AgNPs has been carried out by adding 5 ml leaf extract of *B. stipularis* to 250 ml of the Erlenmeyer flask containing 95 ml of 1 mM silver nitrate ($AgNO_3$) solution. Reduction of silver ions to silver nanoparticles was observed visually within the next 30 minutes by the appearance of light yellowish to dark brown color of the reaction mixture indicates the formation of AgNPs in the solution (Figure 1).

Characterization of phytogenic AgNPs

The change in color of the reaction mixture from yellow to dark brown color indicates the bioreduction of silver ions to silver nanoparticles. Formation of AgNPs was confirmed by characteristic absorption spectrum (JascoV-model 670, UV-Vis NIR spectrophotometer) with a resolution of 1 nm, operated at a wavelength of 300 to 700 nm. The nanoparticles solution was centrifuged for 30 minutes at 35000 rpm (Remi R-8C). The obtained solid residues were again centrifuged 2-3 times in 10 ml distilled water. Finally, purified pellets were dried at 60˚C in an oven to obtain powder and further used for FTIR analysis using potassium bromide (KBr) pellets. The pellets were measured at a range between 4000-400 cm^{-1}. XRD analysis was conducted to determine the crystalline nature and phase purity of the AgNPs. The AFM samples were prepared by the hanging drop method, the AgNPs solution placed onto the glass slide to confirm morphology and distance of the nanoparticles. The HR-TEM analysis of AgNPs was carried out to confirm the size and surface morphology of AgNPs.

Test treatment assay

Pea (*Pisum sativum L.)* seeds were obtained from the seed department of University of Agricultural Sciences (UAS), Dharwad. The seeds were surface sterilized 2-3 times with mercuric chloride to remove fungal contaminants and allowed to germinate on moistened filter paper in petridishes at room temperature. When the radical of the germinated seeds reached 0.5 to 1 cm, thirty seeds each were treated with different concentrations of AgNPs separately (4, 8, 12, 16 µg/ml) at the interval of 6, 12, 18 and 24 hours duration. The different concentrations of AgNPs solution were prepared from 100 µg/ml stock solution. The experiments were conducted in triplicate. After completion of each treatment, roots from germinated seeds were immediately cut and fixed in Carnoy's fluid (ethyl alcohol: glacial acetic acid 3:1 v/v) for 24 hours. Then, they were transferred to 70% ethyl alcohol and stored in the refrigerator at 4˚C for further cytological studies.

Scoring of cells

The cytological slides were prepared as suggested by Yanik et al. [49]. The stored root tips were hydrolyzed in 1 N HCl at 60˚C for 5-10 minutes and squashes were made with 2% aceto orcein for 10 min. Five slides were prepared for each treatment. A minimum of 600 cells were counted from both control and treated groups and approximately 1800 cells were scored for mitotic index and chromosomal abnormalities. The mitotic index and chromosomal abnormalities were calculated by using the following formula MI=Number of dividing cells divided by the total number of analyzing cells multiplied by 100 and chromosomal aberrations were calculated as CAs=Number of abnormal cells divided by total no. of dividing cells multiplied by 100. The cytological slides were photographed at 40X magnification with the bright field microscope (Carl Zeiss), assisted by (Axio imager M2) digital camera.

Statistical analysis

The statistical analysis of data was done by using IBM statistical software (SPSS windows software version 20) followed by two-way ANOVA and Tukey test at the significance level of $p<0.05$.

Results and Discussion

UV-vis Spectroscopy

Silver nanoparticles were characterized by using UV-Vis spectroscopy. In the present investigation, the AgNPs were rapidly formed after the addition of 5 ml leaf extract to the 250 ml Erlenmeyer flask containing 95 ml of one millimolar silver nitrate ($AgNO_3$) solution. The color of the reaction mixtures changes from yellowish to brown color which indicates the formation of AgNPs owing to the excitation of surface plasmon resonance [50,51]. The reaction mixture of AgNPs exhibits different absorbance peaks at 415 nm, 414 nm and 413 nm with pH 8, 9 and 10 respectively (Figures 1 and 2). Whereas, a blue shift represents the prominent peak of AgNPs at 413 nm with pH 10, which confirms the findings of previous studies [52-54]. It is evident from the results that the formation of AgNPs primarily depends on the pH of the reaction medium [55]. In basic and neutral pH the rate of formation of AgNPs is higher when compared to acidic pH.

Fourier Transform Infrared Spectroscopy (FTIR)

FTIR analysis reveals the involvement of functional groups present in the leaf extract of *B. stipularis* (Figure 3 and Table 1). The absorption peaks show IR bands at 3444.52, 2923.44, 2854.95, 1630.06, 1421.42, 1383.68, 1191.82, 1113.88, 1044.64 and 618.56 cm^{-1}. The intense peak at 3444.52 cm^{-1} corresponds to N-H/O-H stretching, the peak at 2923.94

Figure 1: (a) *B. Stipularis* leaf (b) Visual observation of AgNPs with different pH.

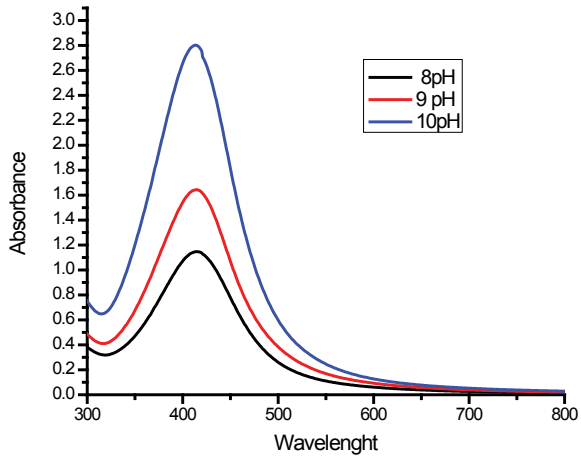

Figure 2: UV-Vis spectrum of AgNPs synthesized by leaf extract of *B. stipularis*.

cm^{-1} corresponds to the methylene antisymmetric vibrational mode. The peak at 2854.95 cm^{-1} is attributed to the presence of methylene symmetric vibrational mode. The band at 1630.06 cm^{-1} represents amide band I and stretching of the carbonyl group. The bands at 1383.68 cm^{-1} and 1191.82 cm^{-1} corresponds -C-O- stretching of the carboxylation ions and -C-O-C- linkages respectively. The bands at 1044.64 cm^{-1} and 618.56 cm^{-1} corresponds C-S stretch (CH2-S) of thiol or thioether/ -C-O-C- bonds and C=C group/ aromatic rings / C=O is stretching in carboxyl groups of proteins respectively. The present study confirms the presence of phytochemicals like alkaloids, flavonoids, tannins, proteins and carboxylic acids and was responsible for bioreduction, capping and stabilization of silver nanoparticles.

X-ray Diffraction (XRD)

X-ray diffraction (XRD) studies were carried out to confirm the crystalline nature of AgNPs synthesized by leaf extract of *B. stipularis*. The diffraction peaks were observed at 2θ values of 38.2˚, 64.6˚ and 77.5˚ which indexed to (111), (220) and (311) sets of lattice planes of face-centered cubic (fcc) of pure silver ions. The result confirms the Joint Committee on Powder Diffraction Standard (JCPDS) card number 04-0783. The FWHM value (111) plane was calculated to determine the mean size of silver nanoparticles using Debye-Scherrer's equation, which showed the crystalline nature of the silver nanoparticles and average size of 12.5 nm. Similar results were reported in AgNPs synthesized by using *Ginkgo biloba* leaf extract (Figure 4).

Atomic Force Microscopy (AFM) and High Resolution Transmission Electron Microscopy (HRTEM)

The structure and surface morphology of silver nanoparticles were ascertained from the atomic force microscopy (AFM). The 2D and 3D images represent different size, shape and height distribution of the biosynthesized silver nanoparticles. The sizes of silver nanoparticles found to vary from 5 to 65 nm and are spherical in shape (Figure 5). The high resolution transmission electron microscopy (HR-TEM) analysis of biogenic AgNPs shows the crystalline nature of the silver nanoparticles with a size range of 15 to 65 nm determined by the measurement scale bar (Figure 6).

Effect of AgNPs on mitotic chromosomes of *Pisum sativum* L.

The cytotoxic and genotoxic effect of biogenic silver nanoparticles was evaluated on the basis of cytological parameters (mitotic index and chromosomal aberrations). Mitotic index is an important parameter and alternative method to determine growth inhibition and genotoxic effect of the cell cycle [56,57]. The root tip meristematic cells of *P. sativum* was exposed to different concentrations (4, 8, 12, 16 µg/ml) of AgNPs solution for 6, 12, 18 and 24 hours duration and results are presented in Table 2. The frequency of dividing cells was observed at all the stages of mitotic cell cycle such as prophase, metaphase, anaphase and telophase. The phase index of prophase is decreased frequently as compared to the control, which indicates the entering percentage of cells into the first phase of mitosis is decreasing [58]. Our data showed that the mitotic index of the control group was found to be highest at 55.43 ± 5.69% and lowest was in 13.99 ± 0.60% at 16 µg/ml concentration of AgNPs suspension for 24 hours duration of treatment, induced a significant reduction in a mitotic index. The results were found to be statistically significant at ($p<0.05$). Our investigation confirms the findings of a cyto-genotoxicity study of Yeken et al. [49] which strongly suggests that the exposure of *A. cepa* root tip cells to CPHE-AgNPs, CBE-AgNPs and AgS induce a significant decrease in mitotic index and increase various types of chromosomal aberrations in a dose and duration dependent manner (Figure 7). The decrease in the mitotic index might be due to the inhibition of cellular proliferative capacity of root cells, which causes slower progression of cells to DNA synthesis or S phase [59-61], blocking in the G2-phase of the cell cycle and averting the cell from entering mitosis [62] and completely destroying the metabolic activities of the cell, which leads to loss of viability and cause cell or DNA damage [63]. Akinboro et al. [64] reported that if the mitotic index is higher than the control, it can be harmful to the cells leading to disordered cell proliferation of meristematic cells. The interaction of silver nanoparticles with human

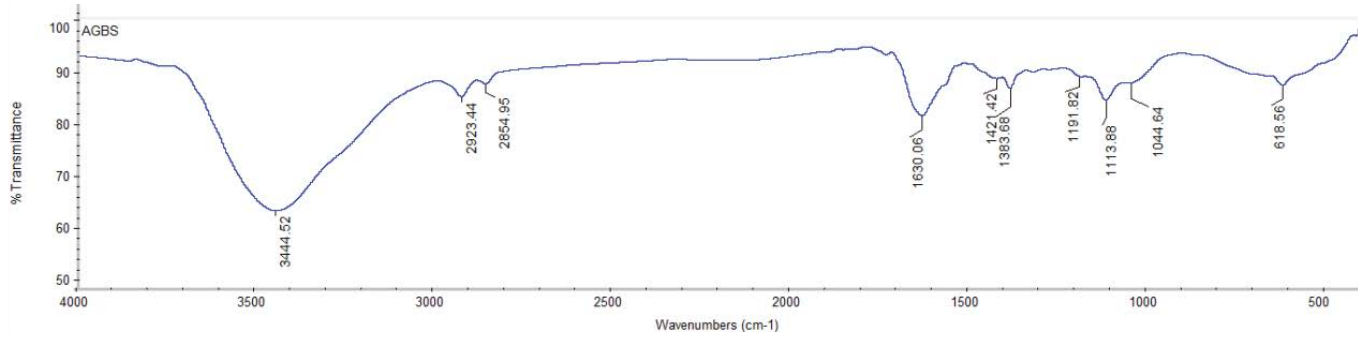

Figure 3: FTIR Spectrum of AgNPs synthesized by leaf extract of *B. stipularis*.

Sl. No.	Absorption peaks of AgNPs	Functional groups
1	3444.52	N-H/O-H stretching
2	2923.44	Methylene anti symmetric vibrational mode
3	2854.95	Methylene symmetric vibrational mode
4	1630.06	Amide band I/Carbonyl stretch
5	1383.68	-C-O- stretching of the carboxylation ions
6	1191.82	-C-O-C- linkages
7	1044.64	C-S stretch (CH2-S) of thiol or thioether/-C-O-C- bonds
8	618.56	C=C group/ aromatic rings/C=O is stretching in carboxyl groups of proteins

Table 1: FTIR absorption peaks and their associated functional groups.

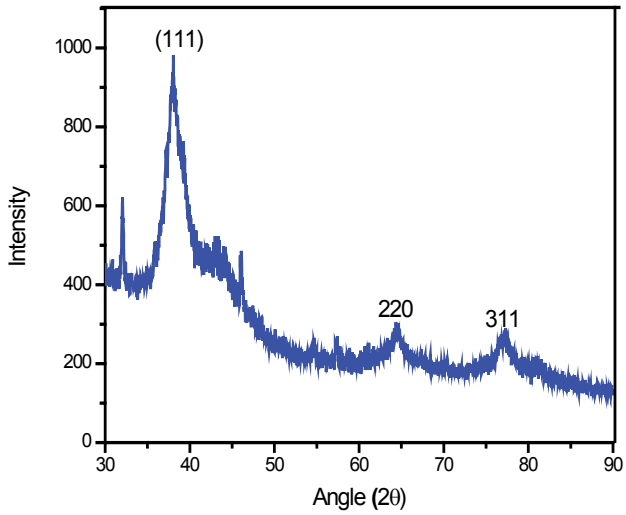

Figure 4: XRD Spectrum of AgNPs synthesized by leaf extract of *B. stipularis*.

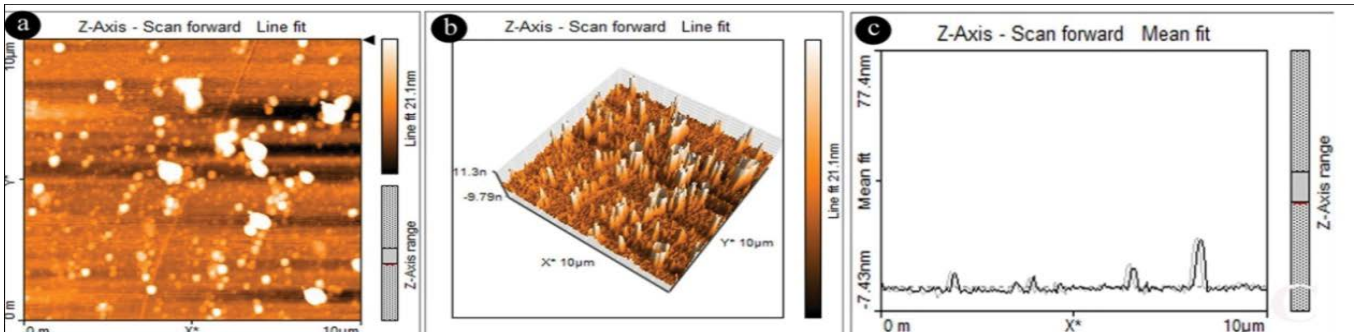

Figure 5: AFM image of AgNPs synthesized by leaf extract of *B. stipularis* (a) Two-dimensional image (b) Three-dimensional image (c) Topography image of AgNPs.

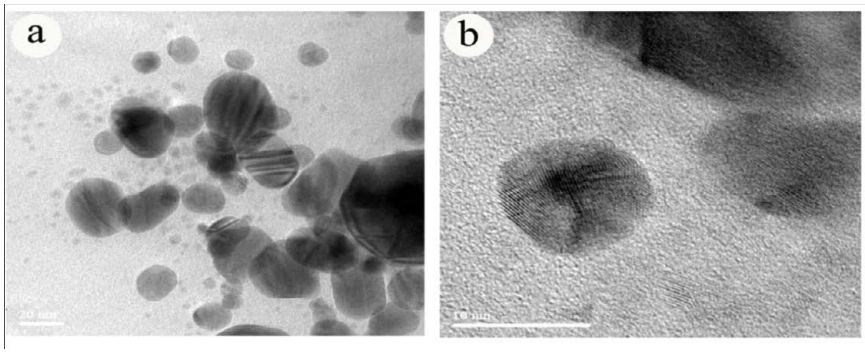

Figure 6: (a & b) HR-TEM image of AgNPs synthesized by leaf extract of *B. stipularis*.

serum albumin elicited binding affinity by bio-physical mechanism which causes significant modification of secondary structure, without any change in its basic structure [65]. Silver nanoparticles inhibited the growth of bacteria and initiate the lipid peroxidation reaction leading to glutathione depletion, disruption of membrane morphology and electron transport chain, which causes DNA damage [66,67]. The silver nanoparticles may bind to the bacterial cell membrane *via* hydrophobic and electrostatic interaction through pinocytosis, which promotes the degradation of cell wall [68]. The tiny sized nanoparticles have a greater surface area causing more toxicity when compared to larger sized nanoparticles [69]. When these small sized nanoparticles enter into the bacterial cell membrane directly or indirectly interacting with nuclear material, resulting in DNA alteration and eventually inactivate the enzymes which are essential for ATP production and DNA replication [70-73]. Present findings confirm the reports of other researchers using different model plant systems viz. *Allium cepa*, [74-78], *Vicia faba* [79], *Triticum aestivum* [49], *Zea mays* [80] and *Drimia indica* [81].

The genotoxic effect of silver nanoparticles on apical meristems of root cells of *P. sativum* have been assayed on the basis of chromosomal

Durations (hrs)	Treatment of AgNP (µg/ml)	MI (%)	Chromosomal bridges	Chromosomal stickness	Vacuolated nuclei	C- Metaphase	Multipolar	Micronucleus	CA (%)
	Control (DI)	55.43 ± 5.69	0.00 ± 0.00	0.00 ± 0.00	0.00 ± 0.00	0.00 ± 0.00	0.00 ± 0.00	0.00 ± 0.00	0.00 ± 0.00
6	4	48.16 ± 6.14	0.22 ± 0.01	1.37 ± 0.38	0.22 ± 0.03	0.11 ± 0.01	0.45 ± 0.21	0.44 ± 0.18	3.54 ± 0.18
	8	46.62 ± 4.44	0.36 ± 0.03	1.77 ± 0.92	0.36 ± 0.03	0.49 ± 0.05	0.77 ± 0.07	0.36 ± 0.03	5.03 ± 0.79
	12	43.75 ± 4.44	0.26 ± 0.02	2.55 ± 0.01	0.26 ± 0.02	0.82 ± 0.04	0.67 ± 0.06	0.28 ± 0.04	5.26 ± 0.97
	16	42.06 ± 4.17	0.58 ± 0.02	1.59 ± 0.70	0.42 ± 0.04	0.57 ± 0.02	0.86 ± 0.04	0.45 ± 0.07	5.94 ± 1.71
12	4	38.18 ± 2.76	0.30 ± 0.02	4.85 ± 1.76	0.29 ± 0.02	0.14 ± 0.02	0.14 ± 0.02	0.45 ± 0.04	7.25 ± 1.39
	8	36.04 ± 4.22	0.31 ± 0.02	4.40 ± 0.73	0.62 ± 0.02	0.31 ± 0.02	0.31 ± 0.02	0.46 ± 0.04	6.76 ± 0.68
	12	32.86 ± 1.87	0.66 ± 0.07	3.50 ± 0.56	0.50 ± 0.05	0.49 ± 0.01	0.82 ± 0.02	0.33 ± 0.02	7.00 ± 1.39
	16	33.92 ± 4.46	0.70 ± 0.06	5.71 ± 0.48	0.51 ± 0.01	0.86 ± 0.02	1.55 ± 0.49	0.69 ± 0.03	10.39 ± 1.36
18	4	31.95 ± 2.65	0.53 ± 0.05	8.04 ± 0.48	0.18 ± 0.03	0.71 ± 0.03	0.89 ± 0.03	0.70 ± 0.02	11.27 ± 0.30
	8	30.18 ± 2.47	0.38 ± 0.03	6.54 ± 1.67	0.18 ± 0.02	0.56 ± 0.05	1.33 ± 0.08	0.95 ± 0.03	11.12 ± 1.39
	12	26.32 ± 1.23	1.89 ± 0.05	6.37 ± 0.33	0.85 ± 0.05	0.83 ± 0.03	1.69 ± 0.39	0.83 ± 0.03	13.99 ± 0.47
	16	24.28 ± 3.32	1.45 ± 0.07	8.57 ± 1.11	0.25 ± 0.04	1.48 ± 0.08	1.47 ± 0.74	0.24 ± 0.04	15.32 ± 1.34
24	4	22.14 ± 0.85	0.78 ± 0.03	11.03 ± 1.43	0.27 ± 0.04	1.03 ± 0.04	0.78 ± 0.03	1.29 ± 0.41	16.78 ± 1.22
	8	19.82 ± 2.14	1.10 ± 0.43	10.35 ± 1.44	0.57 ± 0.09	0.84 ± 0.08	1.09 ± 0.95	1.65 ± 0.77	18.15 ± 1.02
	12	19.43 ± 0.80	1.91 ± 0.06	11.87 ± 3.16	1.59 ± 0.05	1.58 ± 0.51	3.82 ± 0.87	2.20 ± 1.37	25.90 ± 1.59
	16	13.99 ± 0.60	2.16 ± 0.02	16.54 ± 3.63	2.97 ± 0.79	2.19 ± 1.90	3.63 ± 0.46	4.32 ± 1.66	36.95 ± 3.15

Table 2: The effect of AgNPs on Mitotic Index (MI) and Chromosomal Aberrations (CAs) in *P. sativum* root tip merstematic cells.

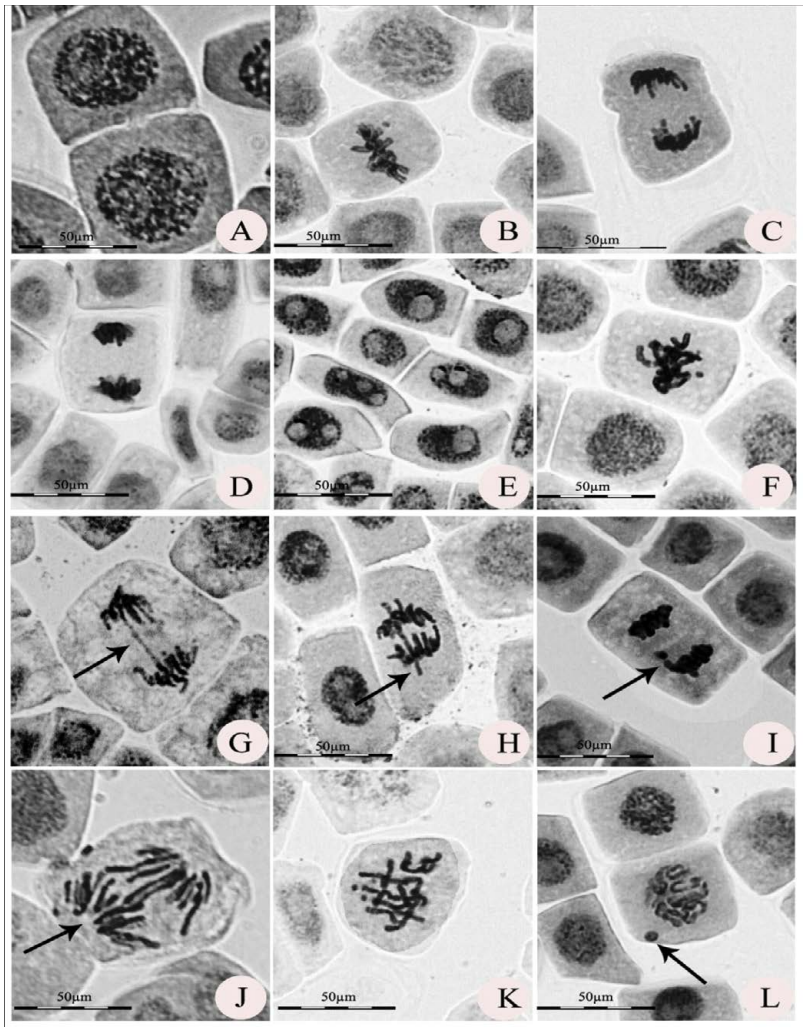

Figure 7: Effect of AgNPs on mitotic chromosomes of root meristem cells of *P. sativum* (A-D) Normal prophase, anaphase, metaphase and telophase (E) Vacuolated nuclei, (F) sticky metaphase, (G) single bridge at anaphase, (H) laggard, (I) telophase with fragment, (J) multipolar anaphase, (K) c-metaphase, (L) micronucleus.

aberrations. There were no chromosomal aberrations in the control. An increase of chromosomal aberrations was recorded at 16 µg/ml concentration (36.95 ± 3.15%) of AgNPs for 24 hours duration of exposure. The results are statistically significant at ($p<0.05$) when compared to control. The induction of chromosomal aberrations was found to be higher at higher concentrations, which has affected cytoplasm and nucleus during cell division [82,83]. Studies of Manna et al. [64] showed an increase in toxicity of engineered nickel oxide nanoparticles on *Allium cepa* root cells along with an increase in genotoxicity at a very low dose.

The cyto-genotoxic effect of biogenic AgNPs was evaluated by analyzing various chromosomal aberrations viz. vacuolated nuclei at prophase, anaphase bridges, chromosomal stickyness, diagonal anaphase, c-metaphase, multipolar anaphase and micronucleus. Vacuolated nuclei were observed in both low and high doses of AgNPs suspension, it appeared that due to the deposition of nanoparticles in intercellular spaces of root cell resulting in chromatin loss and granulated nuclei become vacuolated [84,85]. The chromosomal bridges were occurring due to the presence of dicentric chromosomes and unequal exchange of sister chromatid segments undergoing translocation [86]. The chromosomal stickiness was the most frequent aberration in the present investigation, which arose due to the physiological stress in the form of plasmolysis. However, stickiness may be occurring due to malfunctioning of one or two types of specific nonhistone proteins, i.e. protein-protein interaction which makes chromatids to connect subchromatid bridges. El-Ghamery et al. [87], reported that the diagonal chromosomes may arise due to the effect of silver nanoparticles directly on spindle fibers resulting two sets of chromosomes which do not lie in the same position. The most common type of anomaly occurred in the cell cycle is c-metaphase induced by the interaction of nano-silver with mitotic spindles causing partial suppression of spindle formation and alteration of chromosomes at various stages of the cell cycle [88,89]. Micronucleus or small nuclei are formed from acentric chromosome fragments or whole chromosomes which are not integrated into the nucleus during cell division and are easily detectable in the ensuing stage of interphase [90,91]. It is evident from the present investigation that silver nanoparticles show inhibitory, mitodispersive and turbogenic effect on mitotic chromosomes of root tip meristematic cells of *P. sativum*.

Conclusion

It has been concluded that the leaf extract of *B stipularis* is capable of producing silver nanoparticles from silver nitrate solution and these nanoparticles are relatively stable due to capping aptly by the alkaloids, flavonoids, tannins, proteins and carboxylic acids present in the leaf extract. The prepared biogenic silver nanoparticles are spherical, crystalline and monodispersed with an average size range between 5 and 85 nm. Thus the present study is a simple, safe, efficient, non-toxic and eco-friendly process. Furthermore, the green synthesized AgNPs could enter into the plant system directly causing DNA damage or cell damage in all the phases of cell cycle. The mitotic index was decreased (55.43 ± 5.69% to 13.99 ± 0.60%) at the 16 µg/ml concentration for 24 hours duration of exposure. The present investigation revealed that the mitotic index is inversely proportional and chromosomal aberrations are directly proportional to the concentration and duration of exposure to silver nanoparticles (Figures 8 and 9).

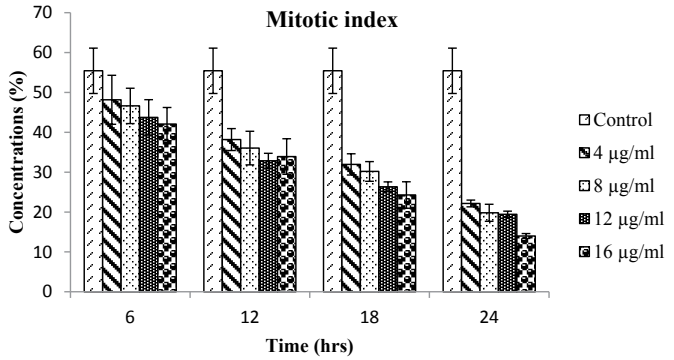

Figure 8: The mitotic index (MI) in root tip meristimetic cells of *P. sativum*, scored at different concentrations (4-16 µg/ml) and at different exposure periods (6-24 hours), found to be statistically significant at ($p<0.05$), when compared to the control.

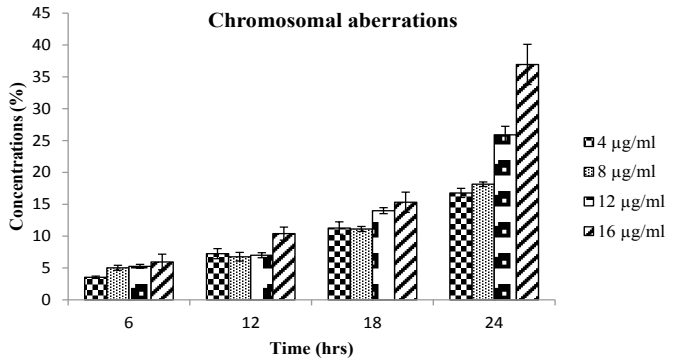

Figure 9: The Chromosomal aberrations (CAs) in root tip meristimetic cells of *P. sativum*, scored at different concentrations (4-16 µg/ml), and at different exposure periods (6-24 hours), found to be statistically significant at ($p<0.05$), when compared to the control.

Acknowledgements

The authors are thankful to the Chairman P. G. Department of Botany, Karnatak University, Dharwad, India, for providing necessary laboratory facilities. Authors also grateful to the University Grant Commission, New Delhi, India. The Authors also thank to USIC, MIT Manipal and IITM Chennai for instrumentation facility. This study is funded by UGC-DSA-I phase programme (No. F.4-29/2015/DSA-I (SAP-II) dated 09-03-2015) of the department. One of the author (A.D) acknowledges the Directorate of Minorities, Government of Karnataka, for awarding Research fellowship.

Conflict of Interest

The author has none to declare.

References

1. Khan M, Naqvi AL, Ahmad M (2015) Comparative study of the cytotoxic and genotoxic potentials of zinc oxide and titanium dioxide nanoparticles. Toxicol Report 2: 765–774.
2. Hussein AK (2015) Applications of nanotechnology in renewable energies-A comprehensive overview and understanding. Renew Sustain Energy Rev 42: 460-476.
3. Hussein AK, Walunj A, Kolsi L (2016) Applications of nanotechnology to enhance the performance of the direct absorption solar collectors. J Therm Eng 2: 529-540.
4. Li D, Li Z, Zheng Y, Liu C, Hussein AK, et al. (2016) Thermal performance of a PCM-filled double-glazing unit with different thermophysical parameters of PCM. Solar Energy 133: 207-220.
5. Hussein AK (2016) Applications of nanotechnology to improve the performance of solar collectors - Recent advances and overview. Renewable and Sustainable Energy Reviews 62: 767-792.
6. Hussein AK, Li D, Kolsi L, Kata S, Sahoo B (2017) A review of nano fluid role to improve the performance of the heat pipe solar collectors. Energy Procedia 109: 417-424.
7. Lakshmanan G, Sathiyaseelan A, Kalaichelvan PT, Murugesan K (2017) Plant-mediated synthesis of silver nanoparticles using fruit extract of *Cleome viscosa* L.: Assessment of their antibacterial and anticancer activity. Karbala Int J Modern sci 4: 61-68.
8. Lampe JW (1999) Health effects of vegetables and fruit: assessing mechanisms of action in human experimental studies. Am J Clin Nutr 70: 475-490.
9. Rahuman AA, Gopalakrishnan G, Ghouse BS, Arumugam S, Himalayan B (2000) Effect of *Feronia limonia* on mosquito larvae. Fitoterapia 71: 553-555.
10. Ledwith DM, Whelan AM, Kelly JM (2007) A rapid, straightforward method for controlling the morphology of stable silver nanoparticles. J Mater Chem 17: 2459-2464.
11. Shay G, Alakhova DY, Kabanov AVJ (2010) Endocytosis of nanomedicines. J Control Release 145: 182-195.
12. Dipankar D, Murugan S (2012) The green synthesis, characterization and evaluation of the biological activities of silver nanoparticles synthesized from Iresine herbstii leaf aqueous extracts. Colloids and Surf B: Biointerfaces 98: 112-119.
13. Vasanth K, Ilango K, Mohankumar R, Agarwal A, Dubey GP (2014) Anticancer activity of *Moringa oleifera* mediated silver nanoparticles on human cervical carcinoma cells by apoptosis induction. Colloids Surf B Biointerfaces 117: 354-359.
14. Patil BN, Taranath TC (2016) *Limonia acidissima* L. leaf mediated synthesis of zinc oxide nanoparticles: A potent tool against Mycobacterium tuberculosis. Int J Mycobacteriol 5: 197-204.
15. Espenti CS, KrishnaRao KSV, Rao KM (2016) Bio-synthesis and characterization of silver nanoparticles using Terminalia chebula leaf extract and evaluation of its antimicrobial potential. Materials letters 174: 129-133.
16. Talib A, Wu HF (2016) Biomimetic synthesis of lotus leaf extract-assisted silver nanoparticles and shape-directing role of cetyltrimethylammonium bromide. J Mol Liq 220: 795-801.
17. Yan-yu R, Hui Y, Tao W, Chuang W (2016) Green synthesis and antimicrobial activity of monodisperse silver nanoparticles synthesized using Ginkgo Biloba leaf extract. Phy Lett A 380: 3773-3777.
18. Mahendran G, Ranjitha Kumari BD (2016) Biological activities of silver nanoparticles from *Nothapodytes nimmoniana* (Graham) Mabb. fruit extracts. Food Sci Hum Wellness 5: 207-218.
19. Sun Y, Yin Y, Mayers BT, Herricks T, Xia Y (2002) Uniform silver nanowires synthesis by reducing $AgNO_3$ with ethylene glycol in the presence of seeds and poly (vinyl pyrrolidone). Chem Mater 14: 4736-4745.
20. Maity D, Bain MK, Bhowmick B, Sarkar J, Saha S, et al. (2011) In situ synthesis, characterization, and antimicrobial activity of silver nanoparticles using water soluble polymer. J Appl Polym Sci 122: 2189-2196.
21. Mathew TV, Kuriakose S (2013) Studies on the antimicrobial properties of colloidal silver nanoparticles stabilized by bovine serum albumin. Colloids Surf B Biointerfaces 101: 14-18.
22. Yin B, Ma H, Wang S, Chen S (2003) Electrochemical synthesis of silver nanoparticles under protection of poly (N-vinylpyrrolidone). J Phys Chem B 107: 8898-8904.
23. Chand R, Rana GC, Hussein AK (2015) On the onset of thermal instability in a low Prandtl number nanofluid layer in a porous medium. J Appl Fluid Mech 8: 265-272.
24. Dimitrijevic NM, Bartels DM, Jonah CD, Takahashi K, Rajh T (2001) Radiolytically induced formation and optical absorption spectra of colloidal silver nanoparticles in supercritical ethane. J Phys Chem B 105: 954-959.
25. Callegari A, Tonti D, Chergui M (2003) Photochemically grown silver nanoparticles with wavelength-controlled size and shape. Nano Lett 3: 1565-1568.
26. Naik RR, Stringer SJ, Agarwal G, Jones S, Stone MO (2002) Biomimetic synthesis and patterning of silver nanoparticles. Nat Mater 1: 169-172.
27. Kolsi L, Hussein AK, Borjini M, Mohammed H, Ben Aissia H (2014) Computational analysis of three-dimensional unsteady natural convection and entropy generation in a cubical enclosure filled with water-Al_2O_3 nanofluid . Arab J Sci Eng 39: 7483-7493.
28. Hussein AK, Ashorynejad H, Shikholeslami M, Sivasankaran S (2014) Lattice Boltzmann simulation of natural convection heat transfer in an open enclosure filled with Cu-water nanofluid in a presence of magnetic field. Nucl Eng Des 268: 10-17.
29. Ahmed S, Hussein AK, Mohammed H, Sivasankaran S (2014) Boundary layer flow and heat transfer due to permeable stretching tube in the presence of heat source/sink utilizing nanofluids. Appl Math Comput 238: 149-162.
30. Xie J, Lee JY, Daniel IC, Ting YP (2007) High-yield synthesis of complex gold nanostructures in a fungal system. J Phys Chem 111: 16858-16865.
31. Kumar B, Smita K, Cumbal L, Debut A (2014) Green Approach for Fabrication and Applications of Zinc Oxide Nanoparticles. Bioinorg Chem Appl 7: 523869.
32. Quester K, Avalos-Borja M, Castro-Longori E (2016) Controllable biosynthesis of small silver nanoparticles using fungal extract. J Biomat Nanobiotechnol 7: 118-125.
33. Khan MZH, Tareq FK, Hossen MA, Roki MNAM (2018) Green synthesis and characterization of silver nanoparticles using *Coriandrum sativum* leaf extract. J Eng Sci Techn 13: 158-166.
34. Hulkoti NI, Taranath TC (2014) Biosynthesis of nanoparticles using microbes- a review. Colloids Surf B Biointerfaces 121: 474-83.
35. Willner I, Baron R, Willner B (2006) Growing metal nanoparticles by enzymes. Adv Mater 18: 1109-1120.
36. Selvi KV, Sivakumar T (2012) Isolation and characterization of silver nanoparticles from *Fusarium oxysporum*. Int J Curr Microbiol App Sci 1: 56-62.
37. Gade A, Gaikwad S, Duran N, Rai M (2013) Screening of different species of Phoma for synthesis of silver nanoparticles. Biotechnol Appl Biochem 60: 482-493.
38. Elamawi RM, Al-Harbi RE, Hendi AA (2018) Biosynthesis and characterization of silver nanoparticles using *Trichoderma longibrachiatum* and their effect on phytopathogenic fungi. Egypt J Biol Pest Control 28:28.
39. Aljabali AA, Akkam Y, Al-Zoubi MS, Al-Batayneh KM, Al-Trad B, et al. (2018) Synthesis of Gold Nanoparticles Using Leaf Extract of *Ziziphus zizyphus* and their Antimicrobial Activity. Nanomaterials 8: 174.
40. Thakur K, Bala I, Rajeshwer, Mamta Devi, Bhatt AK (2017) Evaluation of Effectiveness of Biologically Synthesized Silver Nanoparticles of *Eucalyptus globules* Leaf Extract against Pathogenic and Acne-inducing Bacteria. Journal Nanomed Nanotechnol 8: 2157-7439.

41. Aljerf L, Nadra R (2019) Developed greener method based on MW implementation in manufacturing CNFs. Int J Manuf 15: 269.

42. Sedaghat S, Omidi S (2019) Batch Process Biosynthesis of Silver Nanoparicles, Using Equisetum arvense Leaf Extract. Bioinspired Biomimetic Nano Bio Mater 1-9.

43. Sankaranarayanan AS (1988) Folk-lore medicines for jaundice from Coimbatore and Palghath districts of Tamilnadu and Kerala, India. Anc Sci Life 7: 175-179.

44. Eisai PT (1995) Medicinal herb index in Indonesia. PT Eisai Indonesia. Jakarta. 91.

45. Ngueyema T, Brusotti G, Caccialanzaa G, Vita Finzi P (2009) The genus Bridelia: a phytochemical and ethnopharmacological review. J Ethnopharmacol 124: 339-349.

46. Rama S, Rawat MS, Deb S, Sharma BK (2012) Jaundice and its traditional cure in Arunchal Pradesh. J pharma Scient Innovate 1: 93-97.

47. Sreenivas VK, Jisha VN, Martin KP, Madhusoodanan PV (2011) *Bridelia stipularis*: a new source for anthocyanin production *in vitro*. Acta Physiol Plant 33: 2051-2056.

48. Leme DM, Marin-Morales MA (2009) *Allium cepa* test in environmental monitoring: a review on its application. Mutat Res 682:71-81.

49. Yanık F, Ayturk O, Vardar F (2017) Programmed cell death evidence in wheat (*Triticum aestivum* L.) roots induced by aluminum oxide (Al_2O_3) nanoparticles. Caryologia 2165-5391.

50. Shankar SS, Rai A, Ahmad A, Sastry M (2004) Rapid synthesis of Au, Ag, and bimetallic Au core Ag shell nanoparticles using Neem (*Azadirachta indica*) leaf broth. J Colloid Interface Sci 275: 496-502.

51. Salari Z, Danafar F, Dabaghi S, Ahmad AS (2016) Sustainable synthesis of silver nanoparticles using macroalgae *Spirogyra varians* and analysis of their antibacterial activity. J Saudi Chemical Society 20: 459-464.

52. Mishra PM, Sahoo SK, Naik GK, Parida K (2015) Biomimetic synthesis, characterization and mechanism of formation of stable silver nanoparticles using *Averrhoa carambola* L. leaf extract. Mater Lett 160: 566-571.

53. Amooaghaie R, Saeri MR, Azizi M (2015) Synthesis, characterization and biocompatibility of silver nanoparticles synthesized from *Nigella sativa* leaf extract in comparison with chemical silver nanoparticles. Ecotoxicol Environ Saf 120: 400-408.

54. Roy K, Sarkar CK, Ghosh CK (2015) Rapid colorimetric detection of Hg^{2+} ion by green silver nanoparticles synthesized using *Dahlia pinnata* leaf extract. Green Process Synth 4: 455-461.

55. Edison TJI, Sethuraman MG (2012) Instant green synthesis of silver nanoparticles using *Terminalia chebula* fruit extract and evaluation of their catalytic activity on reduction of methylene blue. Process Biochem 47: 1351-1357.

56. Yumurtaci A, Vardar F, Unal M (2007) Inhibition of barley root growth by Actinomycin D: effects on mitotic activity, protein content and peroxidase activity. Fresen Environ Bull 16: 917-921.

57. Sobieh SS, Kheiralla ZMH, Rushdy AA, Yakob NAN (2016) In vitro and *in vivo* genotoxicity and molecular response of silver nanoparticles on different biological model systems. Caryologia 69: 147-161.

58. Prokhorova IM, Kovaleva MI, Fomicheva AN, Babanazarova OV (2008) Spatial and temporal dynamics of mutagenic activity of water in lake Nero. Inl Water Bio J 1: 1-25.

59. Schneiderman MH, Dewey WC, Highfield DP (1971) Inhibition of DNA synthesis in synchronized Chinese hamster cell treated in G1 with cycloheximide. Exp Cell Res 67: 147-155.

60. Sudhakar R, Gowda N, Venu G (2001) Mitotic abnormalities induced by silk dyeing industry effluents in the cells of *Allium cepa*. Cytologia 66: 235-239.

61. Pandey H, Kumar V, Roy BK (2014) Assessment of genotoxicity of some common food preservatives using *Allium cepa* L. as a test plant. Toxicol Rep 1: 300-308.

62. Van't Hof J (1968) The action of IAA and kinetin on the mitotic cycle of proliferative and stationary phase excised root meristem. Exp Cell Res 51: 167.

63. Manna I, Bandyopadhyay M (2017) Engineered Nickel Oxide Nanoparticle Causes Substantial Physicochemical Perturbation in Plants. Front Chem 5:92.

64. Akinboro A, Bakare AA (2007) Cytotoxic and genotoxic effects of aqueous extracts of five medicinal plants on *Allium cepa* Linn. J Ethnopharmacol 112: 470-475.

65. Beg M, Maji A, Mandal AK, Das S, Aktara M, et al. (2017) Green synthesis of silver nanoparticles using *Pongamia pinnata* seed: Characterization, antibacterial property, and spectroscopic investigation of interaction with human serum albumin. J Mol Recognit 30: e2565.

66. Kumar A, Pandey AK, Singh SS, Shanker R, Dhawan A (2011) Engineered ZnO and TiO_2 nanoparticles induce oxidative stress and DNA damage leading to reduced viability of Escherichia coli. Free Radic Biol Med 51: 1872-188.

67. Ghosh M, Bhadra S, Adegoke A, Bandyopadhyay M, Mukherjee A (2015) MWCNT uptake in *Allium cepa* root cells induces cytotoxic and genotoxic responses and results in DNA hyper-methylation. Mutat Res 774:49-58.

68. Majeed S, Danish M, Zahrudin AHB, Dash GK (2017) Biosynthesis and characterization of silver nanoparticles from fungal species and its antibacte0072ial and anticancer effect. Karbala IntJ Mod Sci 4: 86-92.

69. Carlson C, Hussain SM, Schrand AM, Braydich-Stolle LK, Hess KL, et al. (2018) Unique cellular interaction of silver nanoparticles Size-dependent generation of reactive oxygen species. J Phys Chem B 112: 13608-13619.

70. Baruwati B, Kumar DK, Manorama SV (2006) Hydrothermal synthesis of highly crystalline ZnO nanoparticles: a competitive sensor for LPG and EtOH. Sens Actuators B Chem 119: 676-682.

71. Jayaseelan C, Abdul Rahumana A, Vishnu KA, Marimuthua S, Santhoshkumara T, et al. (2012) Novel microbial route to synthesize ZnO nanoparticles using *Aeromonas hydrophila* and their activity against pathogenic bacteria and fungi. Spectrochimica Acta Part A 90: 78- 84.

72. Mohanty S, Jena P, Mehta R, Patil R, Banerjee B, et al. (2013) Cationic antimicrobial peptides and biogenic silver nanoparticles kill mycobacteria without eliciting DNA damage and cytotoxicity in mouse macrophages. Antimicrob. Agents Chemother 57: 3688-3698.

73. Patil BN, Taranath TC (2018) *Limonia acidissima* L. leaf mediated synthesis of silver and zinc oxide nanoparticles and their antibacterial activities. Microb Pathog 115: 227-232.

74. Kumari M, Mukherjee A, Chandrasekaran N (2009) Genotoxicity of silver nanoparticles in *Allium cepa*. Sci Total Environ 407: 5243-5246.

75. Kumari M, Khan SS, Pakrashi S, Mukherjee A, Chandrasekaran N (2011) Cytogenetic and genotoxic effects of zinc oxide nanoparticles on root cells of *Allium cepa.* J Hazard Mater 190: 613-621.

76. Pesnya DS (2013) Cytogenetic effects of chitosan-capped silver nanoparticles in the *Allium cepa* test. Caryologia: International Journal of Cytology, Cytosystematics Cytogenet. 66: 275-281.

77. Taranath TC, Patil BN, Santosh TU, Sharath BS (2015) Cytotoxicity of zinc nanoparticles fabricated by *Justicia adhatoda* L. on root tips of *Allium cepa* L.-a model approaches. Environ Sci Pollut Res 22: 8611-8617.

78. Yekeen TA, Azeez MA, Lateef A, Asafa TB, Oladipo IC, et al. (2017) Cytogenotoxicity potentials of cocoa pod and bean-mediated green synthesized silver nanoparticles on *Allium cepa* cells. Caryologia: Int J Cytol, Cytosystematics Cytogenet. 70: 366-377.

79. Patlolla AK, Berry A, May L, Tchounwou PB (2012) Genotoxicity of silver nanoparticles in *Vicia faba*: a pilot study on the environmental monitoring of nanoparticles. Int J Environ Res Public Health 9: 1649-1662.

80. Bonea D, Bonciu E (2017) Cytogenetic effects induced by the fungicide Royal Flo to maize (*Zea mays* L.). Caryologia: Int J Cytol, Cytosystematics Cytogenet 70: 2165-5391.

81. Azharuddin D, Taranath TC (2017) Biosynthesis of silver nanoparticles by leaf extract of *Albizia saman* (Jacq.) Merr. and their cytotoxic effect on mitotic chromosomes of *Drimia indica* (Roxb.) Jessop. Environ Sci Pollut Res 24: 25861-25869.

82. Yildiz M, Cigerci IH, Konuk M, Fidan A, Terzi H (2009) Determentation of genotoxic effect of copper sulphate and cobalt chloride in *Allium cepa* root cells by chromosome aberration and comet assays. Chemosphere 75: 934-938.

83. Oyeyemi IT, Bakare AA (2013) Genotoxic and anti-genotoxic effect of aqueous extracts of *Spondias mombin* L, *Nymphea lotus* L. and *Luffa cylindrica* L. on *Allium cepa* root tip cells. Caryologia: Int J Cytol, Cytosystematics Cytogenet 66: 360-367.

84. Huyluoglu Z, Unal M, Palavan-Unsal N (2008) Cytological evidences of the role of meta-topolin and benzyladenine in barley root tips. Adv Mol Biol 1: 31-37.

85. El-Ghamery AA, Mousa MA (2017) Investigation on the effect of benzyladenine on the germination, radicle growth and meristematic cells of *Nigella sativa* L. and *Allium cepa* L. Ann Agric Sci 62: 11-21.

86. Ahmed B, Dwivedi S, Abdin MZ, Azam A, Al-Shaeri M, et al. (2016) Mitochondrial and Chromosomal Damage Induced by Oxidative Stress in Zn^{2+} Ions, ZnO-Bulk and ZnO-NPs treated *Allium cepa* roots. Scientific Rep 7:40685.

87. El-Ghamery AA, El-Kholy MA, El-Yousser A (2003) Evaluation of cytological effects of Zn^{2+} in relation to germination and root growth of *Nigella sativa* L. and *Triticum aestivum* L. Mutat Res 537: 29-41.

88. Mukherjee A, Dhir H, Sharma A (1990) Interaction between essential elements—zinc and iron and metal pollutants-cadmium and lead on cell division and chromosome aberrations in *Valhisneria spiralis* L. Cytologia 55: 405-410.

89. Tanti B, Kumar Das A, Kakati H, Chowdhury D (2012) Cytotoxic effect of silver-nanoparticles on root meristem of *Allium sativum* L. J Biomater Nanobiotechnol 1: 001-008.

90. Fenech M, Kirsch-Volders M, Natarajan AT, Surralles J, Crott JW, et al. (2011) Molecular mechanisms of micronucleus, nucleoplasmic bridge and nuclear bud formation in mammalian and human cells. Mutagenesis 26: 125-132.

91. Dhyevre A, Foltête AS, Aran D, Muller S, Cotelle, S (2014) Effects of soil pH on the *Vicia*-micronucleus genotoxicity assay. Mutat Res Genet Toxicol Environ Mutagen 774: 17-21.